

Self-referencing wavefront sensor

Katie Underwood, J. C. Wyant, C. L. Koliopoulos
Optical Sciences Center, University of Arizona
Tucson, Arizona 85721

Abstract

A modified Smartt point-diffraction interferometer employing phase-shifting electronic phase measurement techniques is described. Special techniques making it possible for the interferometer to give good visibility interference fringes for a large range of input wavefront tilts are discussed. A trade-off between acceptable values of wavefront tilt and light efficiency is presented.

Introduction

The point-diffraction interferometer (PDI)¹ has several advantages for in-situ testing applications. In large optical systems it can conveniently be placed at the end of the optical chain. The reference beam is generated by filtering part of the test beam, and there is no need for a set-up which includes the test optics in some unusual configuration. Another advantage is that the fringe pattern generated by this interferometer represents the wavefront aberration directly. This is unlike most shearing interferometers where complicated calculations are required to characterize the wavefront. However, there are some disadvantages to this system. The fringe visibility becomes poor as varying amounts of tilt are introduced. Also, there is no way to apply phase-shifting techniques in this design.

In the modified PDI the reference beam is generated with polarization normal to the test beam and an Electro-Optical modulator is used to phase shift one of the beams. Standard electronic phase-measurement^{2,3} techniques can then be used to calculate the test wavefront values. Since this system will be used with a fairly powerful source heavy light loss can be tolerated in order to achieve improved visibility fringes for wavefronts having varying amounts of tilt.

Principles

The modified PDI works basically on the same principles as the original Smartt interferometer. In the original design the test beam is focused on the interferometer. A reference beam is generated by diffraction from a small circular aperture in the coating on a plate. The coating attenuates the test beam so the amplitudes of the test and reference beams match giving good contrast fringes. The same result can be achieved by placing a small circular reflective spot on a glass plate. The two designs are compared in Figure 1.

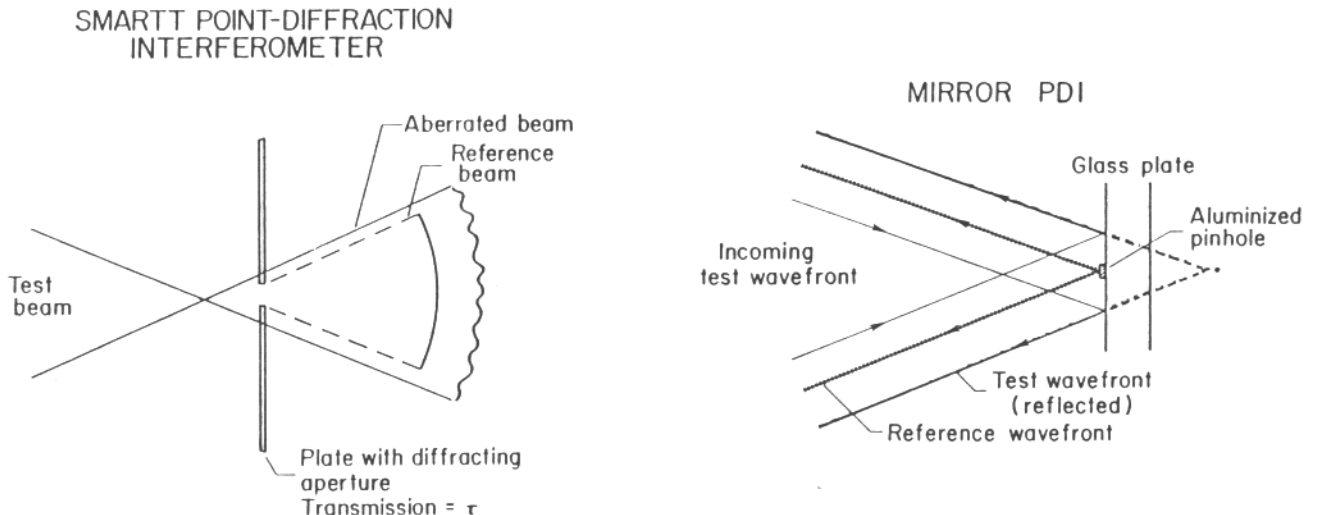


Fig. 1 (left) In the original PDI the test beam falls on a thin plate having a small circular aperture which generates the reference beam. The test beam is attenuated by a coating on the plate. (right) The modified PDI generates the reference by a circular reflective spot.

In the modified PDI a polarizing beamsplitter is used to separate the test beams into two orthogonally polarized beams. Then the polarization of the test beam is rotated 90° by passing twice through a $\lambda/4$ waveplate, and the beam is returned through the beamsplitter. The other beam falls on a reflective circular spot. This spot generates a spherical reference beam whose polarization is also rotated so that this beam is reflected by the beamsplitter. The two beams are still orthogonal and exit the cube together as shown in Figure 2. Now, one polarization is phase-shifted and an analyzer is placed after the E-O modulator to combine the two beams and generate interference fringes on a detector array. The complete setup is shown in Figure 3. A $\lambda/2$ waveplate is placed before the interferometer to rotate the polarization of the incoming beam. This is used to adjust the amount of light going to each arm of the interferometer. This is necessary to match amplitudes in the test and reference beams to yield good contrast fringes.

BEAMSPLITTER PDI

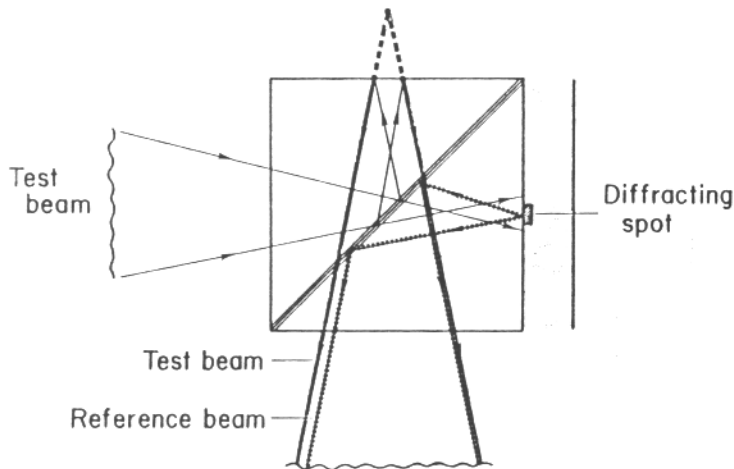


Fig. 2. The cube polarization beamsplitter allows for splitting the reference and test beams into two beams which have orthogonal polarization.

TEST SET-UP

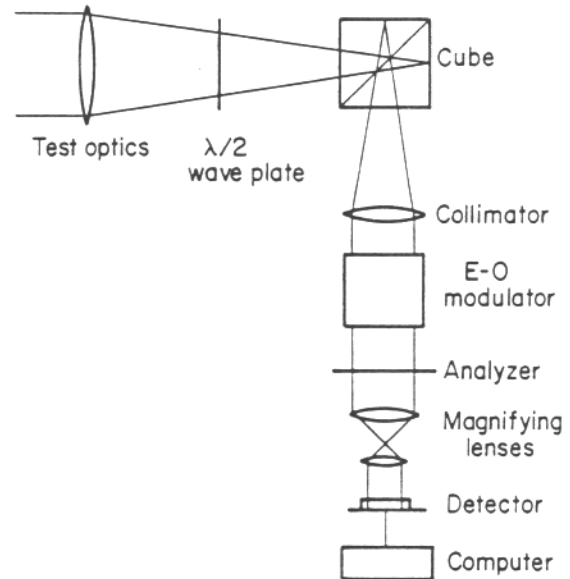


Fig. 3. This shows the cube PDI as used in a test set-up with phase-shifting techniques.

Another advantage to this PDI cube is that it allows for a wide range of test wavefront tilt values. This is achieved by defocusing the test beam from the reflective spot in the reference arm as shown in Figure 4. The defocus introduced into the test beam is eliminated by lengthening the path in that arm. As shown in Figure 5 a glass plate was glued together and placed before the mirror which reflects the test beam. Now, the reference and test beam exit the cube with no defocus between them. Clearly, with a lot of defocus the small reflective spot returns only a small percentage of the light falling on it. This means the $\lambda/2$ waveplate before the cube will be adjusted to send most of the light to the reference arm containing the spot. Consequently, the test arm receives only a small percent of the light.

This modified PDI system is still compact, and can be placed at the focus of a large optical system. It has the added advantages of giving good contrast fringes for a wider range of input tilts and also of allowing for electronic phase measurements. A disadvantage is the large light loss.

Cube construction

The cube PDI is put together as shown in Figure 6. The cube is a $1/2" \times 1/2"$ polarizing beamsplitter which is AR coated on the input and output. All of the components are glued together with optical cement. The test arm of the interferometer consists of several components.

1. A $\lambda/4$ waveplate acts double pass as a $\lambda/2$ waveplate to rotate the test beam 90° and send it through the beamsplitter.
2. The glass plate adjusts for a given amount of defocus.
3. A mirror reflects the test beam.

The reference arm components are similar.

1. A $\lambda/4$ waveplate acts double pass to rotate the reference beam so it will be reflected by the beamsplitter.

2. A glass plate with a small circular reflective spot generates the reference beam.
3. The prism is used to redirect reflections off of the back surface which would cause extra unwanted fringe patterns. This could be replaced by an AR coating on the glass plate.

DEFOCUS INTRODUCED BY THE SYSTEM

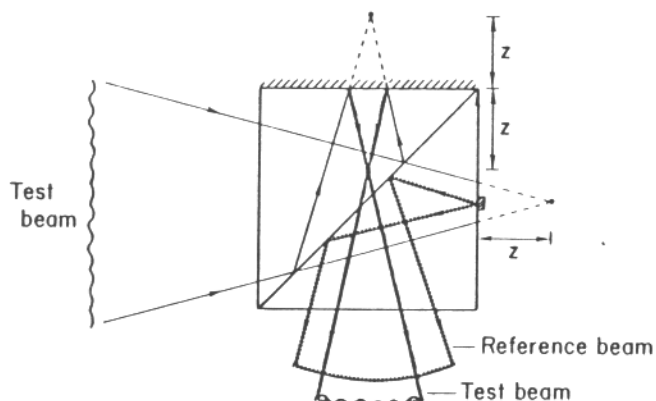


Fig. 4. The reference beam is defocused from the reflective spot introducing defocus between the test and reference beams.

ADJUSTMENT FOR DEFOCUS

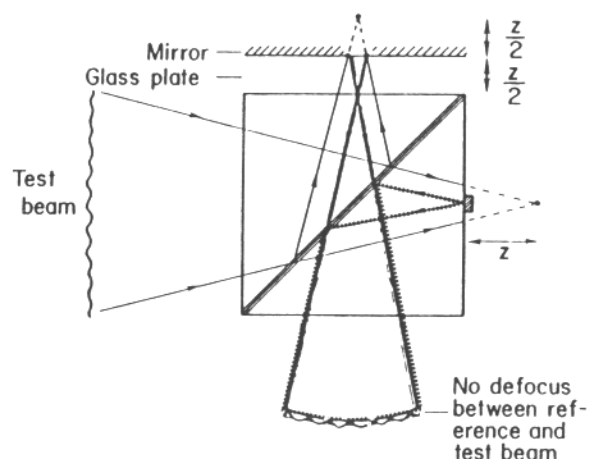


Fig. 5. The addition of a glass plate eliminates the defocus between the two beams.

CUBE CONSTRUCTION

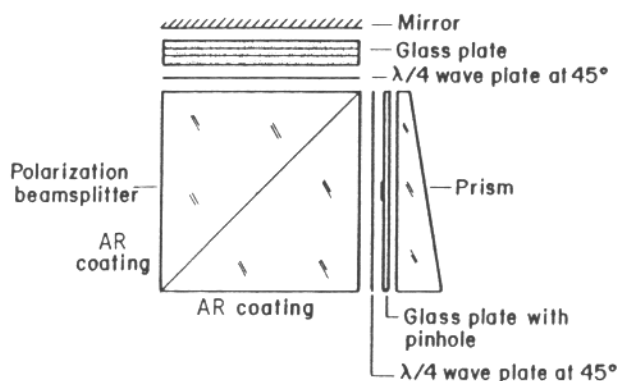


Fig. 6. The components of the cube PDI are glued together as shown above.

The small reflective spot was made in an integrated circuit lab using photoresist techniques. Procedure for making the spot is as follows:

1. The glass plate is coated with aluminum about 1000 Å thick.
2. Positive photoresist (HPR 204) is spun on at 4000 RPM for 30 seconds.
3. This is then prebaked at 100-105° for 30 minutes.
4. A 10 second contact exposure is made from a photo-reduced mask.
5. The glass plate is then developed and the aluminum is etched away except for the spot.
6. The remaining photoresist is stripped off the plate.

The spot size was chosen to be one half the airy disc diameter $\approx \lambda f / \#$ to eliminate aberrations.⁴ Two sizes of spots were made, a 5 micron spot for testing an $f/10$ beam and a 10 micron spot for testing an $f/20$ beam. Pictures of a reflective spot compared with a laser pinhole are shown in Figure 7. A spoke pattern (shown in Figure 8) was placed around the spot to help in locating it and aligning the interferometer.

Calculations

As mentioned before it is necessary to give up light efficiency in order to obtain good contrast tilt fringes. Some discussion of exact numerical values is in order. Figure 9 shows the defocused test beam with and without tilt. For a given amount of acceptable tilt in the reference beam the diameter D of the defocused beam can be expressed as follows:

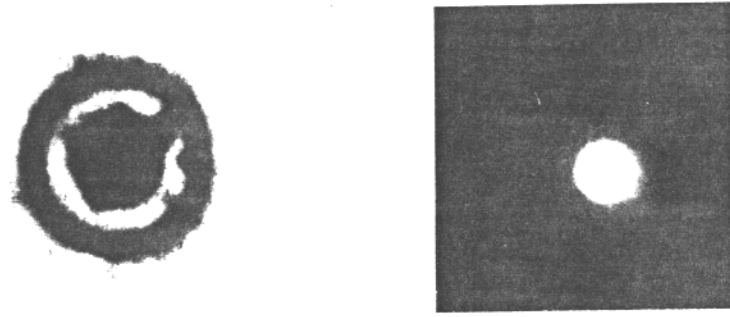


Fig. 7. (left) 10 μm laser pinhole. (right) Aluminized pinhole. Both are shown in reflection.

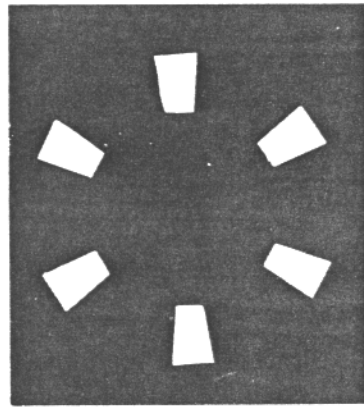


Fig. 8. Target pattern for locating reflective spot.

$$D = d + 2\epsilon \quad (1)$$

where d = diameter of the reflective spot
 ϵ = the shift of the focus of the test beam due to the tilt

also, we know

$$d = \lambda f / \# \quad (2)$$

$$\epsilon = 2 \cdot \lambda \cdot f / \# \cdot W_{011} \quad (3)$$

where W_{011} is the amount of tilt in waves. Substituting these values for d and ϵ into Eq. (1) yields

$$D = \lambda f / \# + 4 \lambda f / \# W_{011} \quad (4)$$

$$= \lambda f / \# (1 + 4 W_{011}) \quad (5)$$

The amount of light, L , returned from the spot can be expressed:

$$L = \frac{d^2}{D^2} \quad (6)$$

$$= \frac{(\lambda f / \#)^2}{(1 + 4W_{011})^2 (\lambda f / \#)^2} \quad (7)$$

$$= \frac{1}{(1 + 4W_{011})^2} \quad (8)$$

A graph of the amount of light returned vs. allowed tilt is shown in Figure 10.

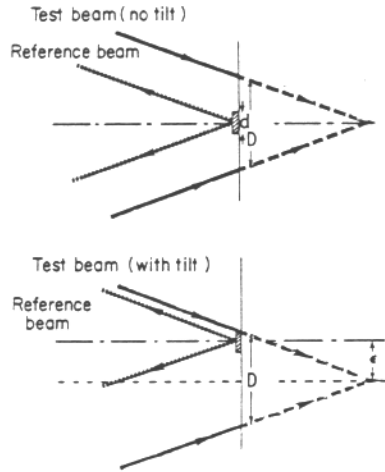


Fig. 9. The defocused test beam yields the same intensity on the reflective spot with or without tilt. This means good contrast fringes for a range of tilt values. However, only a small fraction of the incident light is reflected.

EFFICIENCY vs TILT

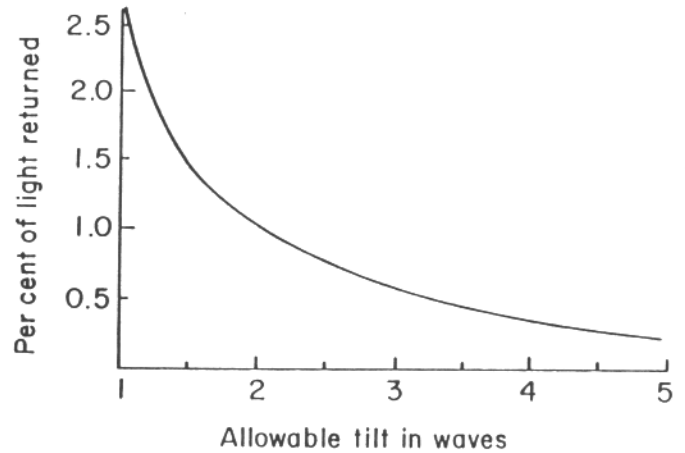


Fig. 10. Shows light efficiency as a function of maximum tilt allowable.

Another point of interest is how much defocus is introduced. The distance from the reflective spot, z , can be expressed in the relationship:

$$\frac{z}{D} = f / \# \quad (9)$$

Therefore,

$$z = D \cdot f / \# \quad (10)$$

$$= \lambda (f / \#)^2 (1 + 4W_{011}) \quad (11)$$

by substituting for D from Eq. (5).

As seen in Figure 5 the glass plate must be of a thickness $z/2$. Using the following equation⁵

$$W_{020} = \frac{z}{-8\lambda (f / \#)^2} \quad (12)$$

it is easy to solve for W_{020} , the amount of defocus in waves. Using z from Eq. (11)

$$W_{020} = \frac{\lambda (f / \#)^2 (1 + 4W_{011})}{-8\lambda (f / \#)^2} \quad (13)$$

$$= \frac{1 + 4W_{011}}{-8} \quad (14)$$

Notice that the amount of defocus is independent of the $f/\#$ being tested and depends only on the amount of tilt to be allowed. However, the thickness of the plates varies linearly with $(f/\#)^2$. Therefore, slower systems require thicker glass. A graph of defocus versus the allowed tilt is shown in Figure 11. The glass thickness in microns can be calculated by multiplying the amount of defocus in waves by approximately $4(f/\#)^2$.

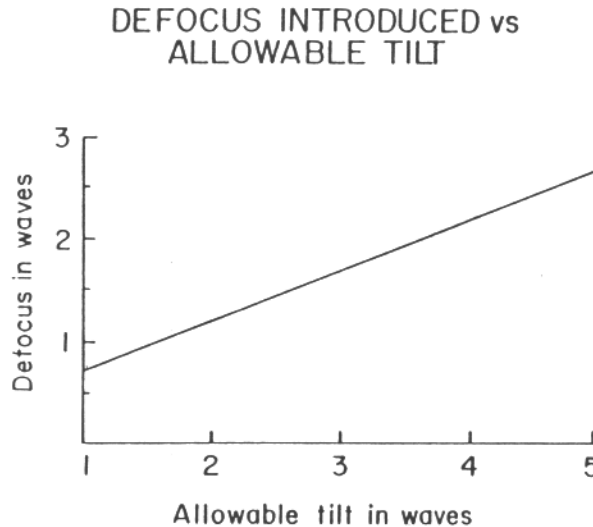


Figure 11. Shows the amount of defocus introduced to accommodate various maximum tilt values.

Although the major light loss occurs at the reflective spot, the final percentage of light that leaves the system depends on several factors and can be expressed as a product:

$$P_0 = \frac{\text{light in}}{\text{light out}} = c \cdot s \cdot a \quad (15)$$

where,

c = the fraction of light that makes it through the cube and $\lambda/4$ waveplate combination
 s = the fraction reflected by the spot
 a = the amount left by the analyzer

Choosing conservative amounts for these:

c = .6 to account for $\lambda/4$ waveplate inaccuracies
 s = .01 to allow for 3 waves of tilt
 a = .3 to account for attenuation in the polarizer

yields

$$P_0 = (.6)(.01)(.3) = .0018 = .18\%$$

This means for a 5 watt laser input the output will be about 9 milliwatts.

Although this is plenty of light there is another problem associated with the small amount of light reflected by the spot. As seen in Figure 6 (showing the cube construction) the waveplate is glued to the glass plate containing the reflective spot. Ordinarily, any reflections at this surface would be negligible. However as the spot reflects less light the amplitudes of these interface reflections are close enough to the amplitude of the spot reflection to interfere and give fairly good contrast fringes. This means that for more defocus on the spot there will also be more visible superfluous fringe patterns. Figure 12 shows interferograms taken with two different amounts of tilt. The top pair were taken with 1 millimeter of glass in the reference arm to adjust for defocus. The bottom were taken with 3 millimeters of glass, or 3 times as much defocus adjustment. While the top interferograms have less high frequency background, they also have less uniform fringe contrast.

Conclusion

This adaptation of the Smartt PDI allows for using phase-shifting techniques in analyzing an in-situ test set-up. It also allows for good contrast fringes over a wide range of input tilts. Problems arise from the many surfaces glued together to make the cube, which yield unwanted reflections.

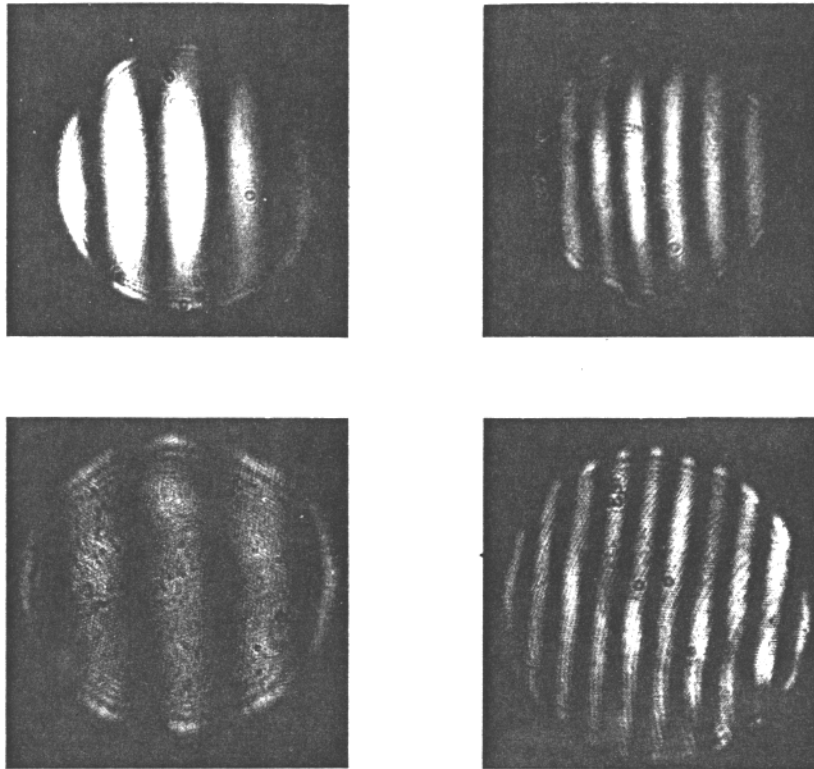


Fig. 12. These interferograms were taken with two different amounts of tilt. The top ones were adjusted for 2.5 waves of defocus at $f/20$. The bottom ones were adjusted by adding more glass for 7.5 waves of defocus at $f/20$.

References

1. R. N. Smartt et al., "Theory and Application of Point-Diffraction Interferometers," Japan J. Appl. Phys., Vol. 14, Suppl. 14-1, pp. 351-356, 1975.
2. J. H. Bruning, "Fringe Scanning Interferometers," in Optical Shop Testing, D. Malacara (ed.), p. 409-436, 1978.
3. Gary E. Sommargren, "Optical Heterodyne Profilometry," Appl. Opt. 20, 610-618, Feb. 15, 1981.
4. Chris L. Koliopoulos and J. C. Wyant, "Spatial Filtering of Aberrations and the Point Diffraction Interferometer," OSA Annual Meeting in San Francisco, October 1978.
5. W. T. Welford, Aberrations of the Symmetrical Optical System, 1974, p. 97.